

Research Journal of Pharmaceutical, Biological and Chemical Sciences

Physical and Mechanical Properties of $Ti_{1-x}Al_xN$ Thin Films Prepared by Different Ion-Plasma Methods.

A L Kameneva^{1*}, V V Karmanov¹, and Dombrovsky I V².

¹Department of Innovative Technologies of Engineering, Perm National Research Polytechnic University, Komsomol'skii pr. 29, Perm, 614990, Russia.

²Closed Joint-Stock Company "Special design Bureau", Open Joint Stock Company for Special Machine Building and Metallurgy «Motovilikhinskiye Zavody», 1905 year str. 35, Perm, 614014, Russia.

ABSTRACT

In this study, the physical and mechanical properties of the $Ti_{1-x}Al_xN$ thin films with $x = 0.11...0.40$ are determined. In addition, their dependence on phase and elemental composition are studied. It is found that with an increase of aluminum content in thin films of up to $x = 0.35...0.40$, all of the thin film's physical and mechanical properties are improved, irrespective of their deposition method. The $Ti_{1-x}Al_xN$ thin film with a volume content of the main hexagonal phase $Ti_3Al_2N_2 \geq 90\%$ has the best physical and mechanical properties: microhardness $H = 35$ GPa, Young's modulus $E = 334$ GPa, elastic recovery $W_e = 76\%$, resistance to elastic failure strain $H/E = 0.11$, and resistance to plastic strain $H^3/E^2 = 0.80$ GPa.

Keywords: $Ti_{1-x}Al_xN$ thin films, physical and mechanical properties, bio-medical material.

**Corresponding author*

INTRODUCTION

The properties of $Ti_{1-x}Al_xN$ thin films, including a high hardness of approximately 28 to 32 GPa, a relatively low residual stress (~ 5 GPa), excellent oxidation resistance, a high hot hardness and a low thermal conductivity [1], make them useful in different industries for improving the antifriction and wear-, heat-, impact- and corrosion-resistant properties of friction assembly unit surfaces. The preservation of the physical, mechanical and thermal properties of thin films in the presence of friction occurs because of the formation of a highly adhesive Al_2O_3 layer on its surface, reducing O_2 diffusion into the thin film and preserving its microhardness at high temperatures [1-2]. The high hardness (~ 37 GPa [3] and 34.7 GPa for $c-Ti_{0.48}Al_{0.52}N$ [4]) and texture of as-deposited thin films are retained for annealing temperatures of up to $950^\circ C$, which indicates a superior stability of this thin film compared with TiN and Ti(C,N) thin films [3]. The oxidation resistance of as-deposited single-phase thin films, both cubic and wurtzite structured, increases with increasing aluminum content, up to $x = 0.7$. The single-phase wurtzite structured thin film, $w-Ti_{0.25}Al_{0.75}N$, shows the best oxidation resistance, with only $\sim 0.7 \mu m$ oxide scale thickness after thermal exposure for 20 h at $850^\circ C$ in ambient air [4].

However, there is a dependence of the structure, thermal stability, oxidation resistance and mechanical properties of the $Ti_{1-x}Al_xN$ thin films on aluminum content [3-7], phase composition and the energy of formation of the thin films [8-17]. In particular, the aluminum content, x , promotes a (200) preferred crystallographic orientation and has a large influence on the hardness of as-deposited thin films [3]. If $x \geq 0.7$, the phase transition from the cubic ($c-AlN$) to the wurtzite ($w-AlN$) structure leads to the mismatch of the molar volumes of $c-Ti_{1-x}Al_xN$ and $w-AlN$, the change of the electronic structure of the $Ti_{1-x}Al_xN$ thin film and its cohesive failure [3,5,6]. Thin films containing Al at the metastable solubility limit, which results in a mixed cubic-wurtzite structure, have the worst oxidation resistance of the $Ti_{1-x}Al_xN$ thin films. For all thin films, a deviation from the linear Vegard-like behavior is predicted for the lattice constants [8]. Whereas the cubic and hexagonal phases exhibit a positive bowing (i.e., the alloy has a larger volume than the mixture of respective binary compounds), the w -phase obeys a negative bowing [8].

Except for microhardness H , the physical and mechanical properties of thin films are typically characterized by the Young's modulus E , the elastic recovery We , the resistance to cracking H/E , and the resistance to plastic deformation H^3/E^2 [9]. It is necessary to investigate the effect that the functional characteristics of the plasma source, the technological and temperature parameters of the thin film deposition and aluminum content in $Ti_{1-x}Al_xN$ thin films has on their physical and mechanical properties.

The purpose of this study was to establish a dependence of the physical and mechanical properties of $Ti_{1-x}Al_xN$ thin film on its microstructure, phase and elemental composition, which change under the influence of the functional characteristics of the plasma source, the technological and temperature parameters of the thin film deposition.

EXPERIMENTAL

The diameter of the upper base of the cathodic arc evaporator's cathode is 37 mm, the diameter of the lower base of the cathodic arc evaporator's cathode is 55 mm, and the height is 44 mm. The diameter of the magnetron's target is 125 mm, and their thickness is 5 mm. The elemental composition of the magnetron's target and cathodic arc evaporator's cathodes are as follows: titanium of the VT-1-00 brand (Ti – 99.5–99.9%; Fe – up to 0.12%; C – up to 0.05%; S – up to 0.08%; N_2 – up to 0.04%; O – up to 0.1%), and aluminum alloy A85 (Al - 99.8%; Fe - up to 0.08%; Si - up to 0.06%; Ti up to 0.01%; Cu up to 0.01%; Zn up to 0.02%).

Substrate preparation: the surfaces of all test samples, i.e., austenitic steel 12H18N10T and flakes from solid alloys VK8, were subjected to ion cleaning and heating using cathodic arc evaporator with a titanium cathode. $Ti_{1-x}Al_xN$ thin film adhesion was improved by depositing a TiN interlayer between the substrate and the thin film; this TiN interlayer was formed in a gas mixture of nitrogen and argon. The thickness of the TiN interlayer varied from 300 to 500 nm, with a total $Ti_{1-x}Al_xN$ thin film thickness of 3.0–5.0 μm . For the production of the $Ti_{1-x}Al_xN$ thin films of different phase and elemental composition, the physical vapor deposition method was varied to be either magnetron sputtering, cathodic arc evaporation or combined method, i.e., the simultaneous usage of the cathodic arc evaporator and magnetron sprayer. A schematic diagram of the deposition device with a location of the cathodic arc evaporators and magnetron sprayers used in experiments is given in Figure 1.

The high voltage supplied to the substrate (U_{high}) was 600 V during ion cleaning-heating. The power supplied to the magnetron sprayer (N) and the nitrogen content in the gas mixture (N_2) were 2.0 kVt and 35 % during the deposition process of magnetron sputtering. The $Ti_{1-x}Al_xN$ thin film's initial temperature (T_{film}) and heating rate of film ($V_{\text{heat.film}}$) were increased by decreasing of the heating rate of substrate ($V_{\text{heat.substrate}}$) from 70 K/min to 45 K/min, by increasing of the gas mixture pressure (P) from 0.8 Pa to 1.2 Pa, and by increasing of the bias voltage supplied to the substrate (U_{bias}) during the deposition of magnetron sputtering from 40 V to 80 V.

The high voltage was 1000 V during ion cleaning-heating. The arc current supplied to cathodic arc evaporator (I_a), current at the focusing and stabilizing coil were matched $I_a = 75$ A, $I_{\text{focusing coil}} = 0.2$ A and $I_{\text{stabilizing coil}} = 0.6$ A. The $Ti_{1-x}Al_xN$ thin film's initial temperature T_{film} and its heating rate $V_{\text{heat.film}}$ were increased by decreasing of the heating rate of substrate ($V_{\text{heat.substrate}}$) from 45 K/min to 10 K/min, by increasing of the gas mixture pressure (P) from 0.5 Pa to 1.0 Pa, and by increasing of the bias voltage supplied to the substrate (U_{bias}) during the deposition of cathodic arc evaporation from 200 V to 280 V.

The technological parameters of the deposition process of combined method are the following: $I_a = 75$ A, $N = 2.0$ kVt, $N_2 = 50$ %, $U_{\text{bias}} = 90$ V and $P = 1.0$ Pa. The $Ti_{1-x}Al_xN$ thin film's initial temperature T_{film} and its heating rate $V_{\text{heat.film}}$ were increased by increasing of the high voltage during ion cleaning-heating process from 600 V to 700 V, and by decreasing of the heating rate of substrate $V_{\text{heat.substrate}}$ from 70 K/min to 20 K/min.

At all variants the thin films were deposited at the rotating substrate. The substrate temperature after ion-bombardment cleaning, temperature of the interlayer TiN and $Ti_{1-x}Al_xN$ thin film after their deposition were measured using a «Termix» infrared non-contact pyrometer.

Phase composition was established using diffraction patterns received from the $Ti_{1-x}Al_xN$ thin film areas using a Shimadzu XRD-6000 diffractometer at $Cu-K_{\alpha}$ radiated emission with an electric potential of 30 kV, current of 20 μ A, an angular spacing of shooting $2\theta = 30-130^\circ$, an interval of 0.1 $^\circ$ and exposition at the point 4 s. Phase changes in the formed $Ti_{1-x}Al_xN$ thin films were estimated by the degree of texturing ($T = I_{\text{max}}/I_{\Sigma}$) of the $Ti_{1-x}Al_xN$ thin film. For the definition of the volume content of each incoming phase (V), the total area of all the XRD peaks was normalized to 100%. Then, the total area of the peaks of the corresponding phase was compared with the total area of all the XRD peaks. For the determination of the titanium concentration, as well as that of aluminum and nitrogen in the $Ti_{1-x}Al_xN$ thin film, a local chemical analysis of its segments was carried out with the use of the field emission electron microscope, Ultra 55, with the prefix EDX-analysis, and a quantitative electron probe microanalysis with the use of x-ray analyzer type, MAR-3, at an accelerating potential difference of 20 kV, a measured current of 20 nA and a sample electrode size of 5 μ m. The cross-sections of the thin film were studied using the field emission electron microscope Ultra 55 [18-21].

The physical and mechanical properties of the $Ti_{1-x}Al_xN$ thin films, including H, E, H/E, H^3/E^2 and We , were determined in accordance with the standard DINENISO 14577-1 method of nanoindentation, which occurred by using a FISCHERSCOPE H100C measuring thin film as well as a mathematical treatment of the received experimental curves series of the load/unload test samples.

RESULTS AND DISCUSSION

During the low-temperature process of *magnetron sputtering* ($T_{\text{film}} = 605$ K and $V_{\text{heat.film}} = 0.1-0.4$ K/min), the $Ti_{1-x}Al_xN$ thin films with $x = 0.11-0.33$, cubic and different hexagonal phases were formed. The formed $Ti_{0.67}Al_{0.33}N$ thin films showed a multi-phase structure with (100) and (101) texture (Figure 2, a). The measured volume contents of the incoming cubic (c-) and hexagonal (h-) phases, h- Ti_2AlN , h- $Ti_3Al_2N_2$, c-TiN, in the $Ti_{0.67}Al_{0.33}N$ thin films were 80.3 %, 16.2 %, 3.5 %, respectively. The aluminum content in the $Ti_{1-x}Al_xN$ thin films decreased as the gas mixture pressure and bias voltage decreased. For example, decreasing the bias voltage up to 40...60 V, resulted in forming a three-phase thin film with c-TiN, c- Ti_3AlN , and h- Ti_2AlN phases and minimum aluminum content of $x = 0.11-0.14$. A maximum increase of the volume content of the h- Ti_2AlN phase, up to 95.9 %, and an increase of the aluminum content in the thin film, up to $x = 0.36$, were caused by a decrease in the substrate heating rate $V_{\text{heat.substrate}}$ up to 45 K/min, and an increase in the film's initial temperature, from 605 K up to 690 K. The maximum degree of the film's texturing formed with short-term thermal pretreatment of the substrate and the low-temperature process of magnetron sputtering is 0.43.

At the temperature process of *cathodic arc evaporation* with $T_{\text{film}} = 670\text{--}735$ K and $V_{\text{heat.film}} = 1.9\text{--}2.2$ K/min, a two-phase $\text{Ti}_{1-x}\text{Al}_x\text{N}$ thin film consisting of h- $\text{Ti}_3\text{Al}_2\text{N}_2$, h- Ti_2AlN phases and a minimum aluminum content of $x = 0.31\text{--}0.32$ was formed. The measured volume content of incoming phases of h- $\text{Ti}_3\text{Al}_2\text{N}_2$ and h- Ti_2AlN were 32.7 % and 67.3 %, respectively. As a result of the T_{film} increasing to 775 K and $V_{\text{heat.film}}$ increasing to 3.5 K/min, the volume content of h- $\text{Ti}_3\text{Al}_2\text{N}_2$ phase increased up to 82 % and aluminum content increased to $x = 0.35$. The $\text{Ti}_{1-x}\text{Al}_x\text{N}$ thin films with $x = 0.38$ and different hexagonal phases were formed when increasing of $V_{\text{heat.film}}$ up to 4 K/min. The measured volume content of incoming phases of h- Ti_2AlN , h- $\text{Ti}_3\text{Al}_2\text{N}_2$, and c-TiN were 3.3 %, 90.5 %, and 6.2 %, respectively. The volume content of the h- $\text{Ti}_3\text{Al}_2\text{N}_2$ phase decreased with decreases in the gas mixture pressure and bias voltage of the substrate. It is determined that the uniform heating of the substrate, increasing an initial temperature T_{film} of the thin film up to 670 K and increasing its heating rate during deposition up to $V_{\text{heat.film}} = 6.0$ K/min by an increase of U_{bias} up to 280 V, creates optimal temperature conditions for the formation of thin films with a maximum (100 %) volume content of the h- $\text{Ti}_3\text{Al}_2\text{N}_2$ phase and a double (107) and (0020) texture (Figure 2, b). The maximum degree of the film's texturing formed after prolonged heating of the substrate and the temperature process of cathodic arc evaporation is 0.83.

At the temperature parameters of *combined method*, $T_{\text{film}} = 605$ K and $V_{\text{heat.film}} = 2.6$ K/min, the multi-phase $\text{Ti}_{1-x}\text{Al}_x\text{N}$ thin films with $x = 0.37$ were formed. The measured volume content of incoming phases, h- Ti_2AlN , h- $\text{Ti}_3\text{Al}_2\text{N}_2$, and c-TiN, were 6.7 %, 90.2 %, and 3.1 %, respectively. The texture was found to be the two competitive with prevailing crystallographic orientation directions (107) and (0020) (Figure 2, c). The increase of the volume content of the h- $\text{Ti}_3\text{Al}_2\text{N}_2$ phase and the aluminum content of the thin film, up to $x = 0.39$, was reached by increasing an initial temperature T_{film} up to 690 K during heating of the substrate, with $U_{\text{high}} = 700$ V, and increasing $V_{\text{heat.film}}$ up to 4.2 K/min. The maximum degree of the film's texturing formed after prolonged heating of the substrate and the temperature process of combined method are the following is 0.74.

It is determined that the microhardness decreases to values of about 21 GPa if formed h- Ti_2AlN , c- Ti_3AlN , and c-TiN phase. This decrease is also valid for the $\text{Ti}_{1-x}\text{Al}_x\text{N}$ thin films with $x=0.11$. The physical and mechanical properties of the $\text{Ti}_{1-x}\text{Al}_x\text{N}$ films: microhardness, Young's modulus, elastic recovery, resistance to elastic failure strain, and resistance to plastic strain increased with an increasing of the aluminum content up to $x = 0.25\text{--}0.38$ and with increasing volume content of h- $\text{Ti}_3\text{Al}_2\text{N}_2$ phase ($V_{\text{Ti}_3\text{Al}_2\text{N}_2}$) up to 76%. The $\text{Ti}_{1-x}\text{Al}_x\text{N}$ thin films on the basis of two hexagonal h- $\text{Ti}_3\text{Al}_2\text{N}_2$ and h- Ti_2AlN phases that are in the phase equilibrium have good physical and mechanical properties.

The physical and mechanical properties of the formed $\text{Ti}_{1-x}\text{Al}_x\text{N}$ thin films with $x=0.25\text{--}0.38$ and $V_{\text{Ti}_3\text{Al}_2\text{N}_2} \geq 76$ % is shown at Figure 3,a as a function of the volume contents of incoming h- $\text{Ti}_3\text{Al}_2\text{N}_2$, h- Ti_2AlN , h- Ti_3AlN , and c-TiN phases, and aluminum content in the $\text{Ti}_{1-x}\text{Al}_x\text{N}$ films.

The elastic recovery, resistance to elastic failure strain, and resistance to plastic strain begins increases when the volume content of the h- $\text{Ti}_3\text{Al}_2\text{N}_2$ phase rises up to 90% and aluminum content rises up to 26,5 at. % ($x=0.38$).

The microhardness and Young's modulus of $\text{Ti}_{1-x}\text{Al}_x\text{N}$ thin films strongly depends on the volume content of h- $\text{Ti}_3\text{Al}_2\text{N}_2$ phase and the aluminum content of the film. Fig. 3,a shows that the microhardness and Young's modulus of $\text{Ti}_{1-x}\text{Al}_x\text{N}$ thin films increased with increasing of aluminum content in the film, and reached an optimal values if Al=28.7 at. % ($x=0.4$). This increase is also valid when the volume content of the h- $\text{Ti}_3\text{Al}_2\text{N}_2$ phase rises. Similar results were also found by other authors (see e.g. the recent reviews [1,3,8] by PalDey, Holec, and Hörling and references therein).

Aluminum has only a slight effect on the thin film's resistance to elastic failure strain H/E because the values of H and E increase with the amount of aluminum in the thin film (the dynamic determined by this change in properties corresponds to the results [1]; see Figure 3,a).

The value of the resistance to plastic strain (H^3/E^2) of the $\text{Ti}_{1-x}\text{Al}_x\text{N}$ thin film depends on the volume content of h- $\text{Ti}_3\text{Al}_2\text{N}_2$ and h- Ti_2AlN phases, $V_{\text{Ti}_2\text{AlN}}$ and $V_{\text{Ti}_3\text{Al}_2\text{N}_2}$. At a maximum value of $V_{\text{Ti}_2\text{AlN}}$ and $V_{\text{Ti}_3\text{Al}_2\text{N}_2}$, the value of H^3/E^2 reaches 1.31 GPa.

Figure 3,b-d shows the cross-section scanning electron micrographs of the $\text{Ti}_{1-x}\text{Al}_x\text{N}$ thin films formed by magnetron sputtering, cathodic arc evaporation and the combined method at an optimal technological and

temperature parameters. Figure 3, b shows the cross-section micrographs of the $Ti_{0.64}Al_{0.36}N$ thin film based on 95,9 % of Ti_2AlN phase formed by the magnetron sputtering in the vertical direction from the substrate. The cross-sectional observation indicates that the sputtered $Ti_{1-x}Al_xN$ thin film has a column structure. The columns of the $Ti_{1-x}Al_xN$ thin film are estimated to be 70 nm in diameter (Fig. 3,b). The $Ti_{0.6}Al_{0.4}N$ thin films with x = 0.40, (107) and (0020) texture formed by the cathodic arc evaporation shows a dense columnar structure with a more abrupt column boundary than in the $Ti_{0.64}Al_{0.36}N$ thin film formed by magnetron sputtering (Fig. 3,c). The columns of the $Ti_{1-x}Al_xN$ thin film are estimated to be 20 nm in diameter. Cathodic arc evaporation formed thin films with high levels of adhesion become more compact and dense as well as macroparticle- and pore-free at the optimal combination of the technological and temperature parameters. It can be seen that by the combined method, at the optimal combination of the technological and temperature parameters, a dense columnar structure is formed with column of 50 to 100 nm in diameter (Fig. 3, d). The film is continuous and dense.

It is determined that the $Ti_{1-x}Al_xN$ thin film formed on homogeneously heated substrates at an optimal the technological parameters, depending on the type of plasma source, technological parameters, the volume content of h- $Ti_3Al_2N_2$ phase and the aluminum content, has different physical and mechanical properties (table). The maximum value of the physical and mechanical properties were $H = 36$ GPa; $E = 382$ GPa; $W_e = 76$ %; $H/E = 0.10$; $H^3/E^2 = 1.31$ GPa for the $Ti_{1-x}Al_xN$ thin film with x=0.4 with just a single-phase h- $Ti_3Al_2N_2$ structure, and column of 20 nm in diameter. This is in good agreement to the literature indicating a hardness maximum for single-phased films with x=0.4–0.7 [1-3]. Possible reason of increasing of the physical and mechanical properties of the formed $Ti_{1-x}Al_xN$ thin films might be the decrease of the crystallite diameter to values, which might result in an increasing role of grain boundary sliding while determining mechanical properties [22].

Table: Physical and mechanical properties of the $Ti_{1-x}Al_xN$ thin film depending on its phase and elemental composition and type of ion-plasma method

Deposition method	T_{film}, K	$V_{heat.film}, K/min$	$V_{Ti_2AlN}, \%$	$V_{Ti_3Al_2N_2}, \%$	$V_{TiN}, \%$	$V_{AlN}, \%$	x (Al)	H, GPa	E, GPa	H/E	$H^3/E^2, GPa$	$W_e, \%$
Magnetron sputtering	690	0.4	95.9	4.1	-	-	0.36	32	351	0.10	0.79	68
Cathodic arc evaporation	670	6.0	-	100	-	-	0.4	36	382	0.10	1.31	76
Combined method	690	4.2	-	91.6	5.4	3.0	35	31	314	0.11	0.65	67

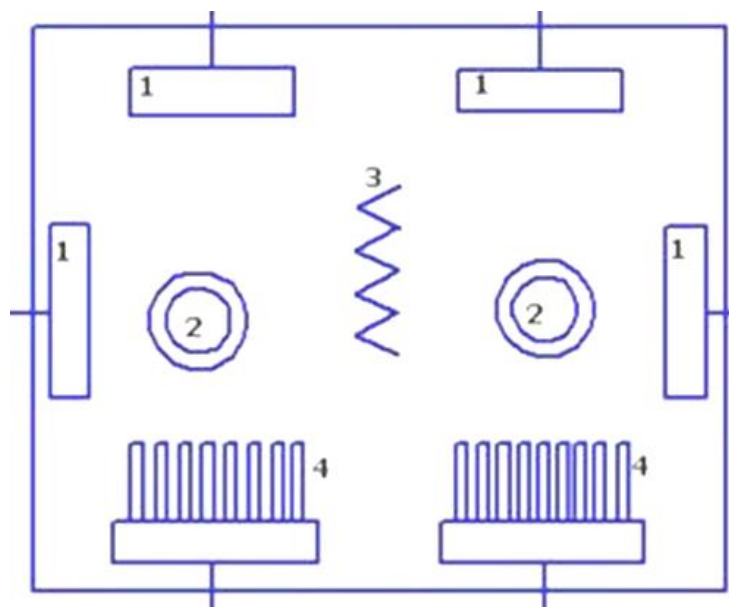


Figure 1: A schematic diagram of the deposition device with a location of the cathodic arc evaporators and magnetron sprayers used in experiments.

Functional knots of the deposition device: 1–magnetron sprayer, 2 – cathodic arc evaporator, 3 – the resistance heater, 4 – the substrate holder

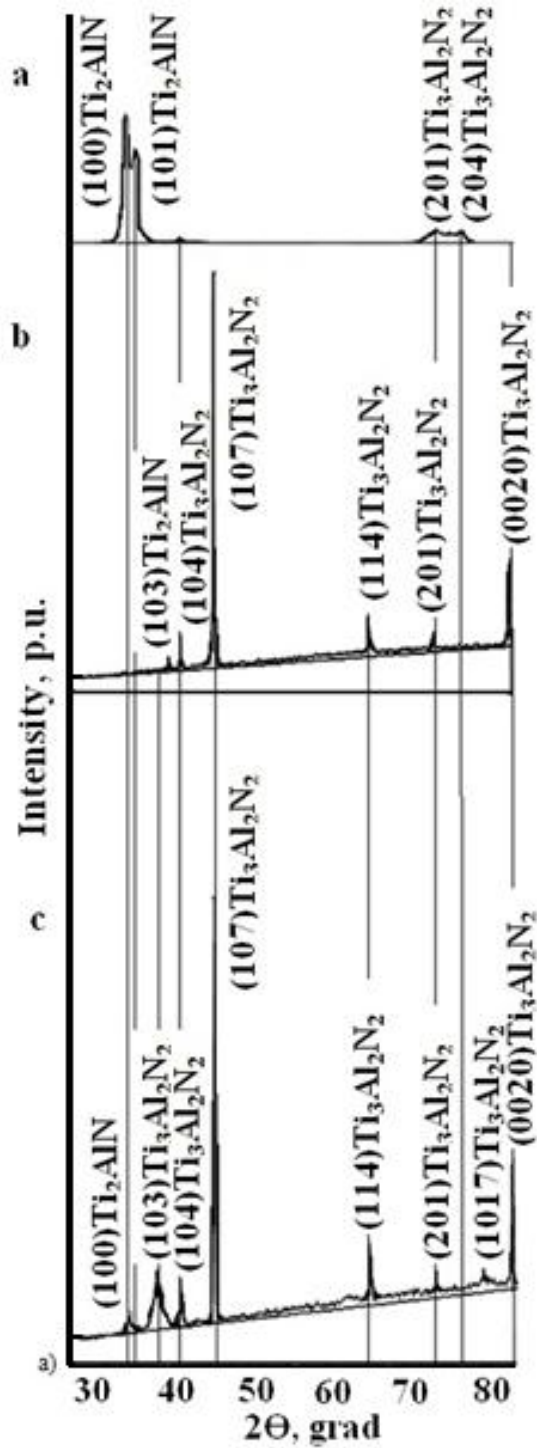
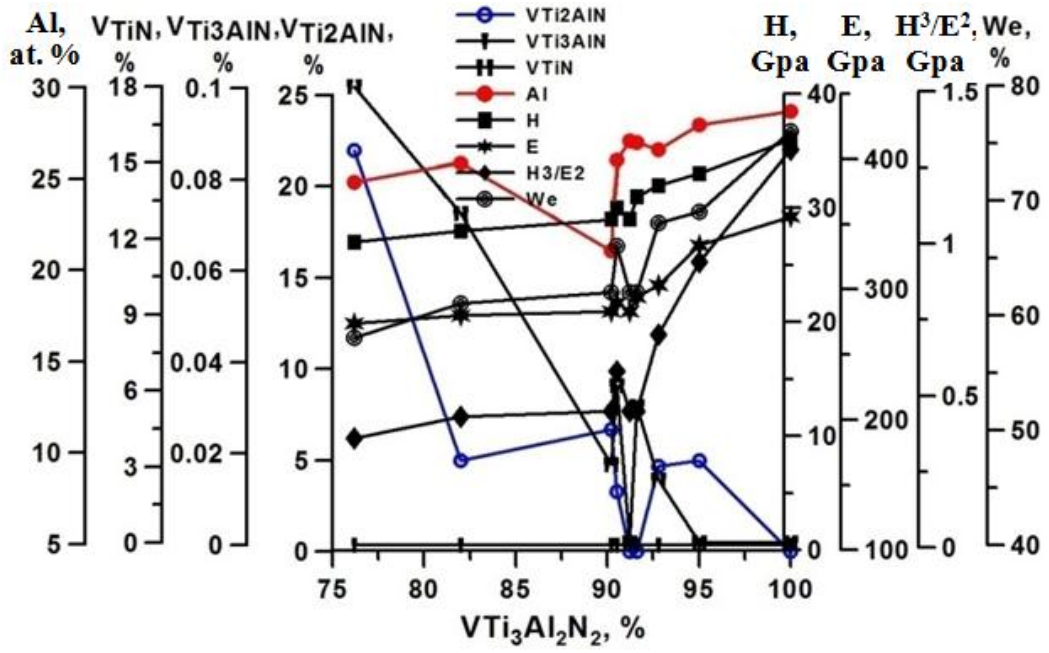
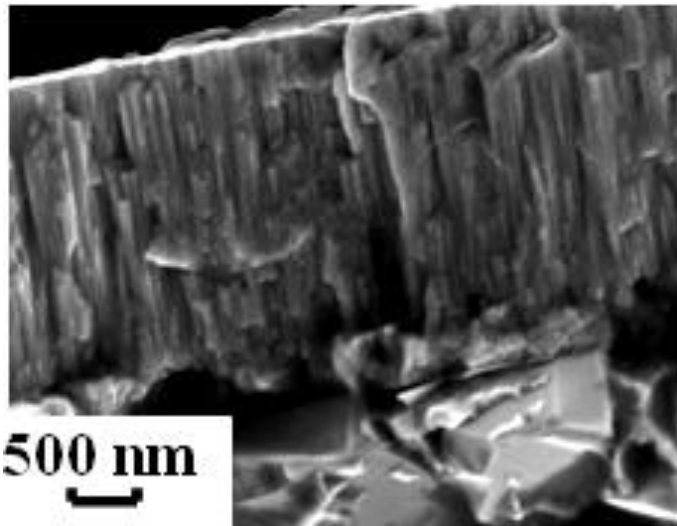


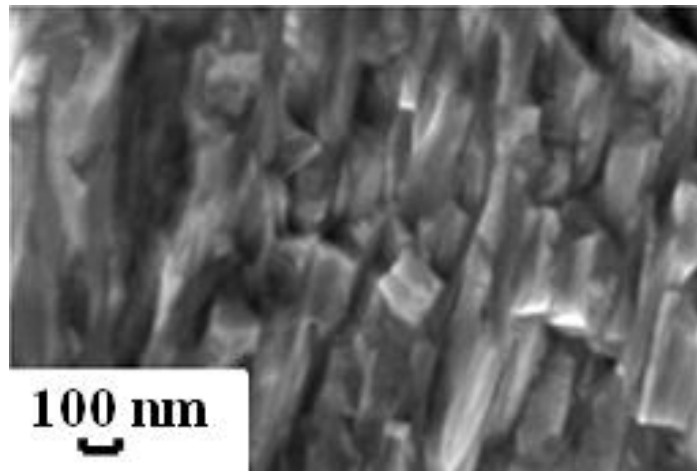
Figure 2: X-ray diffractograms of the areas of $Ti_{1-x}Al_xN$ thin film formed by (a) magnetron sputtering, (b) cathodic arc evaporation and (c) combined method at optimal technological and temperature parameters



a)



b)



c)

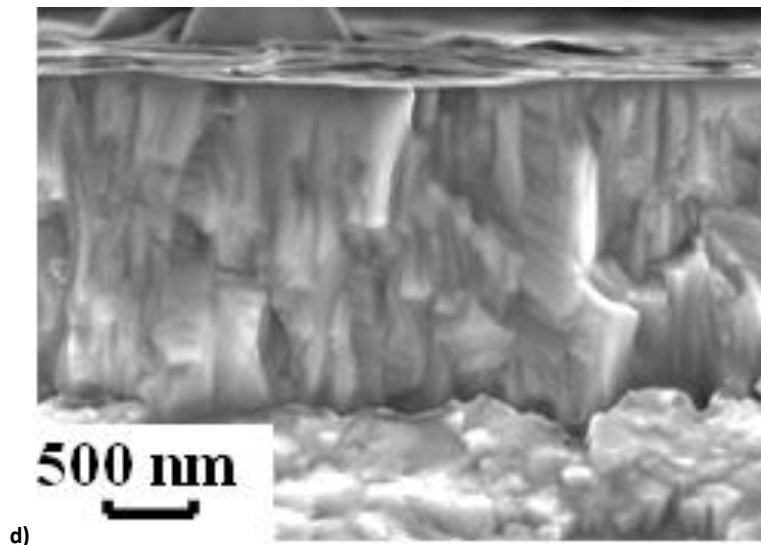


Figure 3: a) The dependence of the physical-mechanical properties of the $Ti_{1-x}Al_xN$ thin film on the volume contents of incoming phases and aluminum content. The cross-section scanning electron micrographs of $Ti_{1-x}Al_xN$ thin films formed by different ion-plasma methods: b) magnetron sputtering, c) cathodic arc evaporation, d) combined method are the following

CONCLUSIONS

The regularities of changes in the physical and mechanical properties of the $Ti_{1-x}Al_xN$ thin films were established under the influence of the volume contents of incoming phases, aluminum content in the films, and microstructure of the film.

First established the role of each incoming phase and a combination of phases, areas for priority crystallographic orientation, and type of texture of the $Ti_{1-x}Al_xN$ thin films in the formation of their physical and mechanical properties.

It was shown that the maximal increase of film heating rates during the process of deposition accelerates plasma chemical reactions and creates optimal technological and temperature parameters for the substrate preparation and formation process of $Ti_{1-x}Al_xN$ thin films with maximum aluminum content and volume content of $h-Ti_3Al_2N_2$ and phases. An increase of aluminum content to $x=0.4$ contributes to an increase of the film's density and an improvement of physical and mechanical properties for the $Ti_{1-x}Al_xN$ thin film. All physical and mechanical properties of the formed $Ti_{1-x}Al_xN$ thin films are improved by increasing the $h-Ti_3Al_2N_2$ volume and reducing of the diameter of crystallites.

The results indicate that it is possible to obtain a high value of hardness for films based on a single-phase $h-Ti_3Al_2N_2$ structure and $x = 0.4$. The value of Young's modulus of a film depends on the value of volume content of $h-Ti_3Al_2N_2$ and $h-Ti_2AlN$ phases in the $Ti_{1-x}Al_xN$ thin films. At a maximum volume content of $h-Ti_3Al_2N_2$ phase, the film Young's modulus value is at minimum and closer to the Young's modulus value of a substrate from austenitic steel 12H18N10T. At a maximum volume content of $h-Ti_2AlN$ phase, the film Young's modulus value is at a maximum and closer to the Young's modulus value of a substrate from solid alloys VK8. At a high film hardness and a minimum value of film the Young's modulus, the thin film's resistance to cracking is optimal.

It was revealed that thin films with a maximum $h-Ti_3Al_2N_2$ phase content on homogeneously heated substrates at optimal technological parameters of the cathodic arc evaporation have the best physical and mechanical properties, which are as follows: $H = 36$ GPa; $E = 382$ GPa; $W_e = 76$ %; $H/E = 0.10$; $H^3/E^2 = 1.31$ GPa. Major performance of $h-Ti_3Al_2N_2$ phase in the growth of resistance and preservation of the physical and mechanical properties of the substrate due to its superior thermal stability compared with other possible combinations formed phases in the $Ti_{1-x}Al_xN$ thin film.

The microstructure of the $Ti_{1-x}Al_xN$ thin film, regardless of its deposition method, is sensitive to the deviation of any of the technological parameters when considering the short-term thermal preparation of the substrate. It has been shown that, for reducing the negative consequences from fabrication with the cutting tool and friction pairs on the process of thin films formation, stress relieving and stabilization of the structure, for each $Ti_{1-x}Al_xN$ thin film–substrate pair, there is an optimal heating temperature and rate of change during the deposition process at which the formation of $Ti_{1-x}Al_xN$ thin film with a complex of high physical and mechanical properties occurs. The physical and mechanical properties of the $Ti_{1-x}Al_xN$ thin film can be controlled by changing the construction, material, preparation technique of the substrate, method and the temperature parameters of the intermediate layers' deposition.

Technological methods for improving the physical-mechanical properties of thin films under optimal technological parameters include uniformly heating the substrate and keeping the optimum temperature and initial rate of heating during the thin film deposition constant. The primary ways to improve the physical-mechanical properties of the thin film under optimal technological parameters are a uniform heating of the substrate and an optimum initial temperature and rate of heating during the deposition process.

ABBREVIATIONS

U_{high} - high voltage supplied to the substrate during ion cleaning and heating,	T_{film} - film's initial temperature,
U_{bias} - bias voltage supplied to the substrate during deposition process,	$V_{heat, film}$ - heating rate of the film,
N - power supplied to the magnetron,	$V_{heat, substrate}$ - heating rate of the substrate,
N_2 - nitrogen content in the gas mixture,	E - film Young's modulus,
P - gas mixture pressure,	W_e - film elastic recovery,
I_a - arc current,	H/E - film resistance to cracking,
T - film degree of texturing,	H^3/E^2 - film resistance to plastic deformation,
	V - volume content of incoming phase, $V_{Ti_3Al_2N_2}$ - volume content of $Ti_3Al_2N_2$ phase.

ACKNOWLEDGMENTS

Work is performed in Perm National Research Polytechnic University with support of the Russian Ministry of Education and Science (contract № 02.G25.31.0068 from 23.05.2013 as part of measures to implement the decisions of the Russian Government № 218).

REFERENCES

- [1] S PalDey, SC Deevi. J. Mat. Sci. Eng. A 2003;342(1):58.
- [2] O Knotek, M Böhmer, T Leyendecker, F Jungblut. Mat Sci Eng A 1988;105–106(2):481.
- [3] A Hörling, L Hultman, M Odén, J Sjöln, L Karlsson. Surf Coat Tech 2005;191(2–3):384.
- [4] L Chen, J Paulitsch, Y Du, PH Mayrhofer. Surf Coat Tech 2012;206(11-12):2954.
- [5] PH Mayrhofer, A Hörling, L Karlsson, J Sjöln, T Larsson, C Mitterer and L Hultman. Appl Phys Lett 2003;83(10):2049.
- [6] C Höglund, Growth and Phase Stability Studies of Epitaxial Sc-Al-N and Ti-Al-N Thin Films: Dissertation. Linköping University, Sweden, 2010, 98.
- [7] A Hörling, L Hultman, M Odén, J Sjöln, L Karlsson. Vac Sci Tech A 2002;20(5):1815.
- [8] D Holec, R Rachbauer, L Chen, L Wang, D Luef, PH Mayrhofer. Surf Coat Tech 2011;206(7):1698.
- [9] DV Shtanskiĭ, SA Kulinich, EA Levashov, JJ Moore. Phys Solid State 2003;45(6):1177.
- [10] TB Massalski, H Okamoto, PR Subramanian, L Kacprzak, WW Scott. "Binary Alloy Phase Diagrams", 2nd ed. ASM International, Materials Park, OH, 1990, Ohio, 1410.
- [11] W Jeitschko, H Nowotny, F Benesovsky, Monatshefte für Chemie, Monatshefte für Chemie 1963;94(6):1198.
- [12] JC Schuster, J Bauer. Solid State Chem 1984;53(2):260.
- [13] MW Barsoum, L Farber, I Levin, A Procopio, T El-Raghy, AJ Berner. Am Ceram Soc 1999;82(9):2545.
- [14] MW Barsoum, T El-Raghy, AT Procopio. Metall Mater Trans A 2000;31(2):373.
- [15] L Hultman, G Håkansson, U Wahlström, JE Sundgren, I Petrov, F Adibi, JE Greene. Thin Solid Films 1991;205(2):153.
- [16] Y Tanaka, TM Gür, M Kelly, SB Hagstrom, T Ikeda. Thin Solid Films 1993;228(1-2):238.
- [17] HA Jehn, S Hoffmann, V-E Rückborn, W-D Münz. Vac Sci Technol A 1986;4(6):2701.



- [18] A Kameneva. Russian journal of Non-ferrous metals 2013;54(6):541.
- [19] A Kameneva. Izvestiya vuzov. Powder metallurgy and functional coatings 2011;4:41.
- [20] A Kameneva, V Karmanov 2013;546:20.
- [21] V Antsiferov, A Kameneva. Russian journal of Non-ferrous metals 2007:48(6):485.
- [22] K Kutschej, P H Mayrhofer, M Kathrein, P Polcik, R Tessadr, C Mitterer Surf Coat Tech 2005;200:2358.